Express Polymer Letters Vol.18, No.6 (2024) 607–622
Available online at www.expresspolymlett.com
https://doi.org/10.3144/expresspolymlett.2024.45

Research article

Photomechanical effect in “side-chain” polyimides with low content of azopyridine chromophore

Jolanta Konieczkowska[1*], *Klaudia Nocoń-Szmajda*[1], *Agnieszka Ciemięga*[2]

[1]Centre of Polymer and Carbon Materials, Polish Academy of Sciences, 34 M. Curie-Sklodowska Str., 41-819 Zabrze, Poland
[2]Institute of Chemical Engineering, Polish Academy of Sciences, 5 Baltycka Str., 44-100 Gliwice, Poland

Received 6 January 2024; accepted in revised form 18 March 2024

Abstract. The paper presents the photomechanical effect generated in new azo side-chain polyimides synthesized through a post-functionalization strategy involving the Mitsunobu reaction. Prepared azo polyimide foils were irradiated by a 405 nm diode-laser beam (intensity, I = 100 mW/cm^2; polarization, E||x) for the generation of the photomechanical effect. Despite the low content of azo chromophore (substitution of the hydroxyl group was in the range of 7–35%) and thick cantilevers (thickness ~35 μm), bending angles were in the range of 30–40°. Thermal unbending was not observed for 12 months after turning off the excitation light. Our investigation showed that, despite the low content of azo chromophore, it is possible to achieve photodeformation under polarized light. To the best of our knowledge, this is the first example of the photomechanical response of azo pyridine polymers.

Keywords: *amorphous polymer, shape memory polymer, photoactive polymer, functional polymer, optical activity*

1. Introduction

Polyimides (PIs) constitute a diverse category of heat-resistant materials known for their remarkable combination of mechanical and thermal properties, thermo-oxidative stability, distinctive electrical characteristics, high radiation resistance, and favourable processability [1]. This versatility allows for the application of polyimides across various industrial domains, notably in photonics, optoelectronics, microelectronics, aerospace (as protective coatings for space applications), passivation layers in lithium-ion batteries, liquid crystal displays, digital isolators, gate insulators for organic electronics, high-voltage capacitors, and printed circuit board technologies, among others [2]. The introduction of azo groups (phenyl rings linked by an N=N double bond) into the polyimide structure imparts a novel property to the material, namely, photosensitivity. The exposure of azo polymers to polarized light (with a wavelength within the range of polymer absorption) induces the *trans-cis-trans* reorientation of azo chromophores and the perpendicular reorientation of their long axes to the polarization of the excitation beam [3]. Consequently, an initially isotropic polymer material transforms into an anisotropic one, giving rise to photoinduced dichroism, birefringence, and the formation of diffraction gratings [4–7]. Additionally, the material exhibits macroscopic mass migration, manifested as a sinusoidal deformation of the polymer film surface referred to as surface relief gratings (SRGs) [5–7] and as the deflection of free-standing films, denoted as the photomechanical effect [8].

The photomechanical effect observed in polymer films, commonly referred to as ‘cantilevers’, manifests as their deflection under irradiation by polarized light [9]. When azo films are irradiated with polarized light of a wavelength within the absorption range of the material (typically UV light), there is an

---

[*]Corresponding author, e-mail: jkonieczkowska@cmpw-pan.pl

increase in the *cis*-isomer population and the reorientation of the *trans* form orthogonal to the incident light's linear electric field vector. A parallel polarized beam aligned with the long axis of the polymer foils induces the perpendicular reorientation of azo chromophores and results in deflection towards the laser source. The unbending of the free-standing films can be achieved by altering the polarization of the laser beam relative to the long axis of the foil. The movements of the cantilevers arise from the strong attenuation of light absorbed by azobenzene moieties, creating a strain gradient across the sample [8, 9].

The photoresponse of azo materials depends on various factors, including the dimensions of the sample (especially thickness), irradiation conditions (intensity of the excitation light, polarization wavelength, position of the wavelength relative to the maximum absorption of azo polymer), the chemical structure of the material (azo group concentration, manner of their incorporation into the macromolecule, type of substituent in the azobenzene group, presence of flexible or bulky groups in the main body of the polymer), and physicochemical properties (thermal and mechanical properties, free volume, morphology, density, and the formation of intra- and inter-molecular interactions). The photogenerated movement of thin foils of azo materials finds applications in various devices, such as optically manipulated arms and azo robots [10–14], micropipettes [15], light-driven micromotors [16, 17], polymer oscillators [18], and photo-controlled ON/OFF currents [19].

The photomechanical movement of azo cantilevers is a well-established phenomenon in liquid crystalline materials and elastomers [8, 9]. Mechanical responses induced by laser irradiation have been observed in various amorphous azo polymers, including homopolyimides, copolyimides [12, 20–23], polyimide gels [24], polyamides [9], poly(amic acid)s [24], and star polyimides [25]. Among amorphous azo polyimides, the photogenerated bending of cantilevers has been predominantly investigated for "main-chain" polyimides [9, 20–23, 25–34]. However, the study of the photomechanical effect is less prevalent for other categories of azo polyimides, such as "T-type" [35] or "guest-host" azo systems [36, 37]. Side-chain azo polyimides, in particular, have received limited attention, with an in-depth examination reported solely in the work of Sun *et al*. [38]. In their study, the polymer featured bulky CF_3 groups in the main chain, and a derivative of azobenzene was attached in the side chain via the flexible $–O–C_{11}H_{22}–$ group. The bending angle of a ~20 µm thick cantilever reached 70° when exposed to 365 nm light (intensity $I = 70$ mW/cm^2, polarization E‖x). The azo polyimide was employed in the fabrication of a light-controlled opening and closing mechanism for a cubic box.

In this study, polyimides featuring covalently bonded azo dye were synthesized using the post-functionalization method based on the Mitsunobu reaction. The synthesis involved reacting polyimide matrices containing –OH groups with 4-[4-(6-hydroxyhexyloxy)phenylazo]pyridine. A comprehensive literature review revealed a notable absence of articles describing azo pyridine polymers in the context of their photomechanical response. The motivation for undertaking this study stemmed from the results obtained in our previous works, wherein a significantly faster *cis*-*trans* isomerization in the dark was demonstrated [39], along with improved thermal properties of azo pyridine polymers in comparison to azobenzene analogues [40]. The azo polyimides presented in this work were characterized with respect to their capacity for *trans*-*cis* photoisomerization, dark *cis*-*trans* relaxation in a solid state, and the generation of the photomechanical response.

2. Experimental section

2.1. Materials

4,4′-(hexafluoroisopropylidene)diphthalic anhydride (6FDA) – H0771, 3,3′-dihydroxybenzidine (HAB) – D2312, 2,3,5,6-tetramethyl-1,4-phenylenediamine (4MPD) – T1457 were obtained from Tokyo Chemical Industry Co., Ltd (Fukaya, Japan). 4,4′-bisphenol A diphtalic dianhydride (BPADA) – 478032, triphenylphosphine (TPP) – T84409, Diethyl azodicarboxylate (DEAD) – 225541, 1,2-dichlorobenzene (ODB) – 240664, anhydrous *N*-methyl-2-pyrrolidinone (NMP) – 5.89597 *N*,*N*-dimethylformamide (DMF) – 227056 were received from Sigma-Aldrich (Steinheim, Germany). Methanol – FP[67-56-1] was purchased from Avantor Performance Materials Poland S.A. (Gliwice, Poland).

4-[4-(6-hydroxyhexyloxy)phenylazo]pyridine was synthesized and characterized in previous work [41]. HAB and 4MPD diamines were dried overnight before use in a vacuum oven at 80 and 100 °C, respectively. DMF was vacuum-distilled before use.

2.2. Measurements

2.2.1. Polymer characterization

Proton nuclear magnetic resonance (^{1}H NMR) experiments of the investigated materials were carried out on an Avance II UltraShield Q3 Plus Bruker MT 600 MHz spectrometer (Germany). Tetramethylsilane (TMS) and deuterated dimethyl sulfoxide (DMSO-d_6) were used as an internal standard and as a solvent, respectively. The chemical shifts (δ) were recorded in ppm.

Fourier transform infrared spectroscopy-attenuated total reflectance (FTIR-ATR) data were received by using a Nicolet 6700 FTIR apparatus (Thermo Scientific, MA, USA). The FTIR spectra were acquired in the range of 4000–500 cm^{-1}, at the resolution of 0.09 cm^{-1} for 64 accumulated scans. The samples were prepared using potassium bromide (KBr) pallets. The reduced viscosity ($\eta_{\text{red.}}$) was determined at 25 °C for the NMP solution of 0.67 g/dL polymer concentration. The measurements were performed using an Ubbelohde's viscosimeter (k = 0.01148). The absolute density (ρ) was measured using an AccuPyc 1330 Micromeritics helium pycnometer equipped with a 1 cm^3 sample chamber. Before the analysis, the samples were dried at 100 °C for 2 h. Samples were analyzed three times. Each measurement collected data points from 10 cycles of He dosing. Wide-angle X-ray diffraction (WAXD) analysis was performed using an HZG-4 diffractometer (Carl Zeiss, Jena, Germany). The samples were examined working on Bragg geometry of 2θ from 5 to 50° using Ni-filtered Cu-K$_\alpha$ radiation with a wavelength λ = 1.54051 Å. Differential scanning calorimetry (DSC) data were recorded on a TA-DSC 2010 apparatus (TA Instruments, Newcastle, DE, USA). Before the analysis, the azo polyimide samples were vacuum-dried at 100 °C for 24 h. The samples were analyzed with a heating rate of 20 °C/min. The glass transition temperature (T_g) was taken as a midpoint of the heat capacity step change registered in a second run. Thermogravimetric analysis (TGA) was done with a TA TGA55 apparatus with a heating rate of 15 °C/min in a constant stream of nitrogen (25 mL/min) and a temperature range from 25 to 800 °C. The compounds before measurement were dried in an oven at 100 °C for 24 h in a glass vessel. UV-Vis spectroscopy. The measurements of UV–Vis absorption spectra were measured for polymer solutions in NMP (c = 10^{-5} mol/L) and films cast on a glass substrate using a Jasco V-750 (Jasco Inc., Japan). The cell path used for the spectroscopic measurement of the solution was 10 mm. The chromophore loading level of the azo polyimides was determined by the UV–Vis spectroscopy using the Lambert–Beer Law. The degree of the chromophore substitution in the polymer was calculated from the calibration curves obtained from the UV–Vis spectra of the chromophore solution with various concentrations ($1\cdot10^{-6}$–$1\cdot10^{-4}$ mol/L) for the 4-[4-(6-hydroxyhexyloxy)phenylazo]pyridine (equation of the calibration curve was $y = 5.842x - 0.0523$). From the comparison of the peak absorbance of the polymer in solution with the known concentration and the calibration curve, the degree of the functionalization was estimated. The absorbance of azo polymer (c = 10^{-5} mol/L) was 0.1359 for **azo-PI-1**, 0.2520 for **azo-PI-3**, and 0.0787 for **azo-PI-3** at 358 nm ($\lambda_{\max}$ of azo dye in NMP).

2.2.2. Polymer film preparation

The homogenous solutions of polymers in NMP were filtered through 0.45 mm membranes and cast onto clean glass substrates (2×2 cm). Polymer thin films for isomerization measurements were prepared by casting solution onto glass substrates and heating them for 8 h at 100 °C on the heating plate. The residual solvent was removed from the films by heating them for 24 h at 100 °C in vacuum. Free-standing polymer films for photomechanical effect studies were prepared by heating for 8 h at 100 °C on the heating plate and then dried for 24 h at 120 °C in a vacuum.

2.2.3. *Cis-trans* isomerization measurements

The measurements of UV–Vis absorption spectra were measured for polymer films cast on a glass substrate placed in the darkroom for at least 24 h. The *trans-cis* and *cis-trans* reactions were monitored at room temperature (25 °C). The measurement procedure was as follows: in the first step, the absorption spectra of the polymer films were recorded without any irradiation. Then, the *cis*-isomers were generated by 405 nm diode-laser light (intensity, I = 100 mW/cm^2) until reaching the photostationary state. The photostationary state was achieved after 5 min. Increasing the exposure time did not increase the number of *cis*-isomers in the sample compared to the 5 min exposure time. Then *cis-trans* dark-return isomerization at room temperature was monitored by recording changes in the absorption spectrum from 30 min up to 6 days after irradiation of the sample.

By monitoring the changes in the absorbance at the wavelength corresponding to the absorption maximum of the *trans*-form, before and immediately after light irradiation. The conversion efficiency of the *trans*-form to the *cis*-form was determined according to the Equation (1):

$$P = \frac{A_0 - A_t}{A_0} \cdot 100\% \tag{1}$$

where P is content of *cis*-isomers in percent, A_0 and A_t correspond to the normalized absorbance before and after 5 min irradiation, respectively.

2.3. Synthesis of polyimides

BPADA-HAB (PI-1): polyimide was synthesized *via* the one-step polycondensation reaction with the standard procedure described by us previously [42]. The reaction of BPADA dianhydride and HAB diamine was carried out in NMP and ODB mixture to obtain 20% solid concentration (NMP/ODB 4/1 (v/v)) for 3.5 h at 180 °C under reflux and in a nitrogen atmosphere. The polyimide **PI-1** was precipitated in a mixture of methanol/water (2/1, v/v) and purified by a Soxhlet extraction for a few days to remove any reaction solvents. The product was dried in a vacuum oven at 100 °C for several hours.

PI-1: ^{1}H NMR (600 MHz, DMSO-d_6), δ [ppm]: 1.71 (s, CH_3, 6H), 7.19–7.96 (m, ArH, 20H), 10.08 (s, OH, 2H). ATR-FTIR ν [KBr, cm^{-1}]: 3720–3010 broad (–OH); 2969 (CH_2); 1777, 1720 (–C=O in imide); 1443 (–CH_3 deformation); 1318 (–C–N– stretching); 1100, 1076 (–C–O–C stretching); 746 (–C–N– deformation).

6FDA-HAB (PI-2): polyimide was synthesized *via* the two-step polycondensation reaction using an ester-acid method following the standards described by us earlier [43]. The reaction of 6FDA dianhydride derivative and HAB diamine was carried out in a mixture of NMP/ODB (4/1, v/v) with a total solid concentration of 20 wt% for 8 h at 180 °C under reflux and in a nitrogen atmosphere. The polyimide **PI-2** was precipitated in a mixture of methanol/water (2/1, v/v) and purified by a Soxhlet extraction for a few days to remove any reaction solvents. The product was dried in a vacuum oven at 100 °C for several hours.

PI-2: ^{1}H NMR (600 MHz, DMSO-d_6), δ [ppm]: 7.18–8.20 (m, ArH, 12H), 10.06 (s, OH, 2H). ATR-FTIR ν [KBr, cm^{-1}]: 3390–2919 broad (–OH); 1786, 1737 (–C=O in imide); 1380 (–C–N– stretching); 723 (–C–N– deformation).

6FDA-HAB-4MPD 1:1 (PI-3): copolyimide, was synthesized *via* the one-step polycondensation reaction with the procedure described by us [44]. The reaction of a mixture of HAB and 4MPD diamines in a molar ratio of 1:1 and the respective equimolar amount of 6FDA dianhydride was carried out in a mixture of NMP/ODB (4/1, v/v) with a total solid concentration of 20 wt%, for 3.5 h at 180 °C under reflux and in a nitrogen atmosphere. The polyimide **PI-3** was precipitated in a mixture of methanol/water (2/1, v/v) and purified by a Soxhlet extraction for a few days to remove any reaction solvents. The product was dried in a vacuum oven at 100 °C for several hours.

PI-3: ^{1}H NMR (600 MHz, DMSO-d_6), δ [ppm]: 2.09 (s, CH_3, 12H), 7.18-8.24 (m, ArH, 18H), 10.12 (s, OH, 2H). ATR-FTIR ν [KBr, cm-1]: 3750–3010 broad (–OH); 1790, 1710 (–C=O in imide); 1467 (–CH_3 deformation); 1380, 1350 (–C–N– stretching); 720 (–C–N– deformation).

2.4. Synthesis of azo polyimides

Azo polyimides (azo-PIs) were synthesized *via* the Mitsunobu reaction as was described earlier [42]. The polyimide **PI-1**, **PI-2**, or **PI-3** (1 g); 4-[4-(6-hydroxyhexyloxy)phenylazo]pyridine (0.8981 g, 3 mmol); and TPP (3 mmol) were dissolved in NMP at 80 °C and in a nitrogen atmosphere. Next, DEAD (3 mmol) was added dropwise to the mixture, and the Mitsunobu reaction was carried out at 80 °C for 120 h. The azo polyimides **azo-PIs** were precipitated in methanol and purified in a Soxhlet's apparatus for a few days. Products were dried in an oven at 50 °C for 2 h.

azo-PI-1: ^{1}H NMR (600 MHz, DMSO-d_6), δ [ppm]: 1.25–1.63 (m, CH_2, 8H) $OCH_2(\mathbf{CH_2})_4CH_2O$, 1.73 (s, CH_3, 6H), 3.89–4.13 (m, CH_2, 4H) $O\mathbf{CH_2}(CH_2)_4\mathbf{CH_2}O$, 6.95–7.66 (m, ArH, 20H), 7.98 (d, ArH, 4H), 8.75 (d, ArH, 2H), 10.09 (s, OH, 1H). ATR-FTIR ν [KBr, cm^{-1}]: 3708–3136 broad (–OH); 2944 (CH_2); 1778, 1720 (–C=O in imide); 1600 (–N=N–); 1445 (–CH_3 deformation); 1378 (–C–N– stretching); 1103, 1077 (–C–O–C– stretching); 747 (–C–N– deformation).

azo-PI-2: ^{1}H NMR (600 MHz, DMSO-d_6), δ [ppm]: 1.31–1.59 (m, CH_2, 8H) $OCH_2(\mathbf{CH_2})_4CH_2O$, 3.81–4.09 (m, CH_2, 4H) $O\mathbf{CH_2}(CH_2)_4\mathbf{CH_2}O$, 7.08–8.22

(m, ArH, 18H), 8.75 (d, ArH, 2H), 10.07 (s, OH, 1H). ATR-FTIR ν [KBr, cm^{-1}]: 3452–2988 broad (–OH); 2950 (CH_2); 1787, 1736 (–C=O in imide); 1598 (–N=N–); 1378 (–C–N– stretching); 722 (–C–N– deformation).

azo-PI-3: ^{1}H NMR (600 MHz, DMSO-d_6), δ [ppm]: 1.34–1.78 (m, CH_2, 8H) $OCH_2(\mathbf{CH_2})_\mathbf{4}CH_2O$, 2.09 (s, CH_3, 12H), 3.82–4.10 (m, CH_2, 4H) $O\mathbf{CH_2}(CH_2)_4\mathbf{CH_2}O$, 6.94–8.22 (m, ArH, 24H), 8.78 (d, ArH, 2H), 10.08 (s, OH, 1H). ATR-FTIR ν [KBr, cm^{-1}]: 3707–3028 broad (–OH); 2956 (CH_2); 1787, 1727 (–C=O in imide); 1612 (–N=N–); 1463 (–CH_3 deformation); 1381, 1357 (–C–N– stretching); 723 (–C–N– deformation).

3. Results and discussion

In this study, three new "side-chain" azo polyimides (azo-PIs) were synthesized and comprehensively characterized, encompassing thermal, optical, and photomechanical properties. As previously indicated in the Introduction section, the investigation of "side-chain" azo polyimides in the context of photomechanical effect generation has been limited, with only one study identified in the literature [38]. In that study, the azo polymer was prepared through a one-stage pre-functionalization process involving low-temperature polycondensation of commercially available 4,4′-(hexafluoroisopropylidene)diphthalic anhydride (6FDA) and a modified diamine with azo group linkage through a flexible –O–$C_{11}H_{22}$– chain. Consequently, an azobenzene group was attached to each polymer repeat unit. In this work, we synthesized azopolymides with a "side chain" substituting the hydroxyl group not exceeding 35%.

Azo-modified polymers were prepared based on polyimide matrices designated as **PI-1**, **PI-2**, and copolyimide **PI-3**, as illustrated in Figure 1. The precursors were synthesized using 3,3′-dihydroxybenzidine (HAB) and 4,4′-bisphenol A diphtalic dianhydride (BPADA) for PI-1, 4,4′-(hexafluoroisopropylidene)diphthalic anhydride (6FDA) for **PI-2**, or a combination of 6FDA, HAB, and 2,3,5,6-tetramethyl-1,4-phenylenediamine (4MPD) in a 1:1 M ratio for **PI-3** (Table 1). The inclusion of different functional groups, such as ether bridges, fluorine, and methyl groups in the benzene ring, has been shown to alter the polymer morphology, as previously described by our group elsewhere [43, 44]. Azo polyimides, denoted as **azo-PI-1**, **azo-PI-2**, and **azo-PI-3**, were obtained through post-modification using the Mitsunobu reaction (Figure 1). The azo pyridine derivative, 4-[4-(6-hydroxyhexyloxy)phenylazo]pyridine, was covalently linked to the polymer backbone through a flexible alkoxyhexyloxyl group. The degree of hydroxyl group substitution in the polymer chain with the dye was determined using the Lambert-Beer law through UV-Vis spectroscopy. UV–Vis measurements revealed an 18, 35, and 7% substitution of hydroxyl groups for **azo-PI-1**, **azo-PI-2**, and **azo-PI-3**, respectively.

3.1. Characterization of (azo)polyimides

The chemical structures of the obtained polyimides and their azobenzene-functionalized counterparts were verified by the proton nuclear magnetic resonance (^{1}H NMR) and fourier transform infrared spectroscopy (FTIR-ATR) analysis. ^{1}H NMR spectra show characteristic signals of the unsubstituted hydroxyl groups at around 10.00 ppm, aromatic protons in the range of 8.78–6.94 ppm, aliphatic protons from alkoxyhexyloxyl group of the azo substituent in the range of 4.13–3.81 ppm and the range of 1.78–1.25 ppm. In addition, **azo-PI-1** and **azo-PI-3** exhibit signals at around 2.00 ppm which correspond to protons derived from methyl groups. Figure 2 shows the FTIR spectra of the (co)polyimide precursors and their azo-functionalized analogs. The studied polymers show characteristic bands of the imide rings. They exhibit symmetrical (1790–1777 cm^{-1}) and asymmetrical (1737–1710 cm^{-1}) stretching vibrations of the C=O bond, as well as stretching (1381–1378 cm^{-1}) and deformation (747–720 cm^{-1}) vibrations of the C–N bond. The absorption bands of the ether groups for **PI-1** and **azo-PI-1** are observed at ca. 1100 and 1076 cm^{-1} as well as at ca. 1103 and 1077 cm^{-1}, respectively. The absorption bands at ca. 1440 cm^{-1} observed for **PI-1**, **PI-3**, and their functionalized analogs are related to the stretching vibration of methylene groups located in BPADA dianhydride or attached to the benzene ring in 4MPD diamine. The azo chromophore covalently attached to the polyimide structure (**PI-2** and **PI-3**) is associated with an increased absorption band at ca. 2956–2950 cm^{-1}. These bands correspond to the methylene groups in the aliphatic chain of the azo compound, which is observed for **azo-PI-2** and **azo-PI-3**. The decrease of intensity of the absorption band in the range of 3720–3010 cm^{-1} characteristic for stretching vibrational of OH groups is observed for azo-functionalized polymers. It is related to the formation

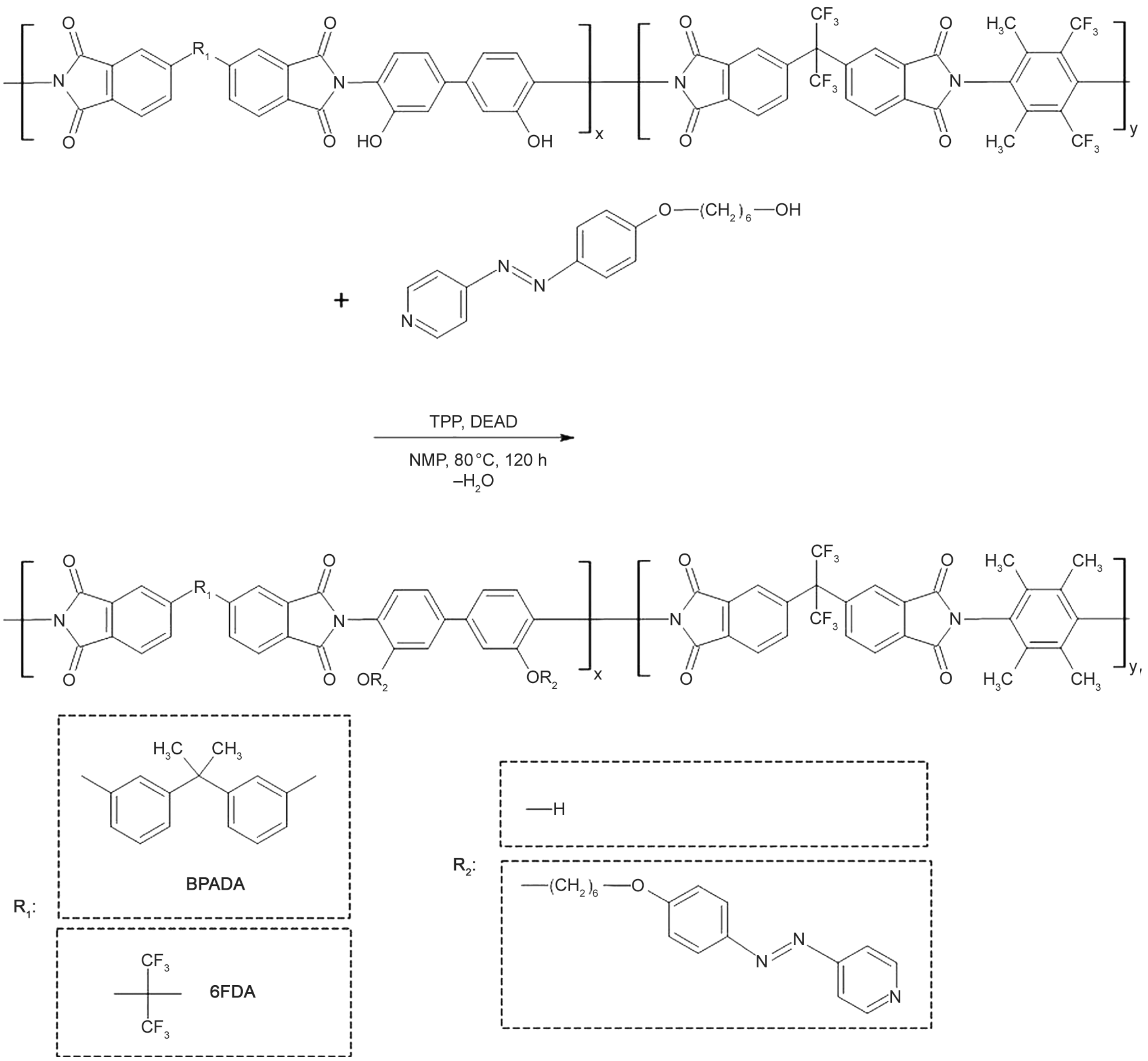

Figure 1. Synthesis route of azo polyimides.

Table 1. Molar fraction of monomers used in synthesis of polyimide matrices.

Polymer code	BPADA	6FDA	HAB	4MPD
	[mol fraction]			
azo-PI-1	1	–	1	–
azo-PI-2	–	1	1	–
azo-PI-3	–	1	0.5	0.5

of the alkoxyl group as a result of the Mitsunobu reaction. Furthermore, all the studied azo-PIs showed additional absorption bands at around 1612–1598 cm^{-1} characteristic of the N=N group.

The viscosity, density, and d-spacing were assessed for both the precursors and the azopyridine-functionalized polyimides, and the pertinent data are compiled in Table 2. In the case of **azo-PI-1** and **azo-PI-2**, the viscosity exhibited no significant change after functionalization with azo groups when compared to their respective PI precursors. A distinct trend was observed for **azo-PI-3**, where the viscosity decreased from 0.67 to 0.51 dL/g following azo modification. High-quality foils were successfully obtained from all azo-PIs. Density measurements of the PIs and azo-PIs, conducted using a helium pycnometer, revealed that the effect of the presence of an azo-side chain on density depended on the flexibility of the polyimide precursor. In the case of **PI-1**, featuring an ether linkage in the main chain, an increase in density was observed, rising from 1.04 to 1.41 cm^3/g. Conversely, for polymers lacking a flexible –O– bond, a reverse dependence was noted. Specifically, for **azo-PI-2** and **azo-PI-3**, density decreased from 1.66 to 1.53 cm^3/g and from 1.71 to 1.58 cm^3/g, respectively.

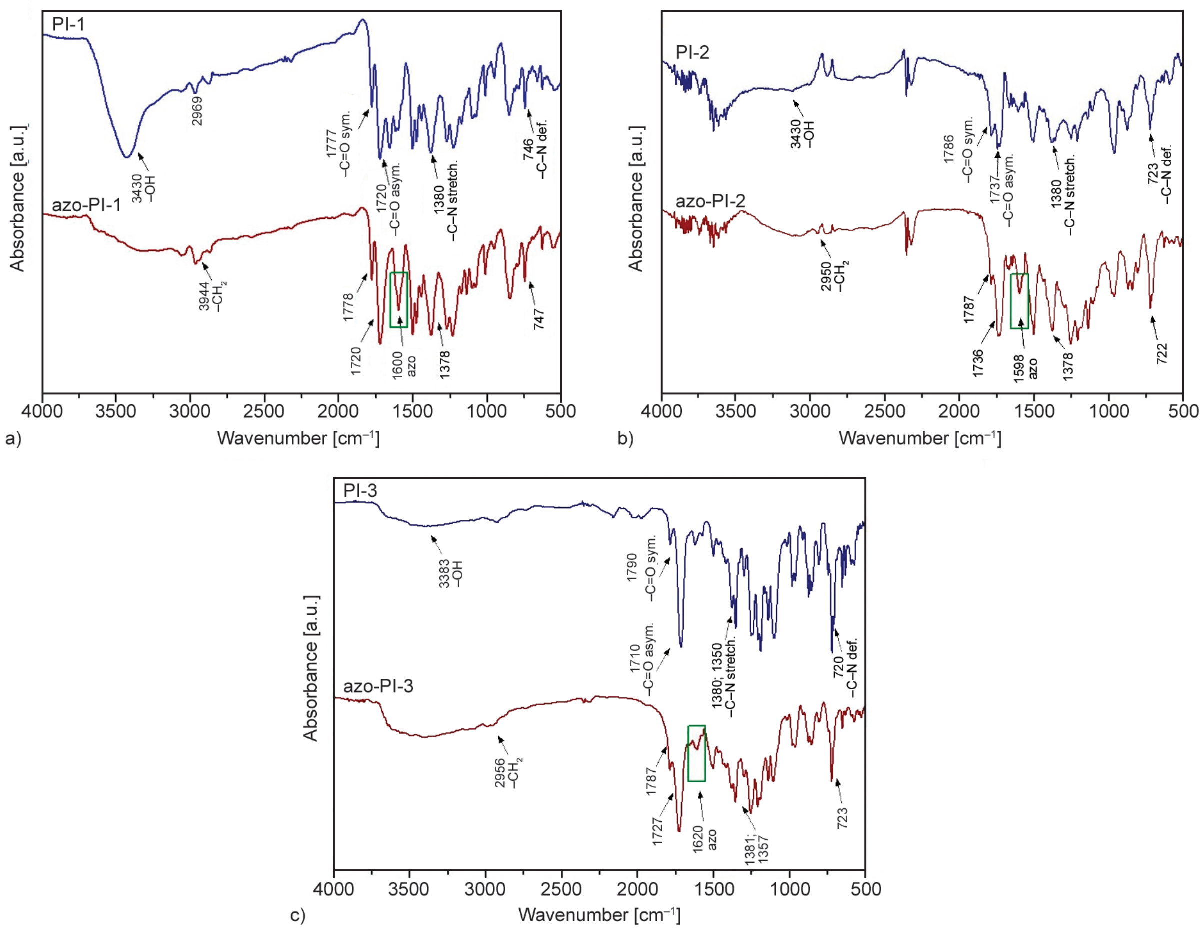

Figure 2. FTIR-ATR spectra of the precursors and azo-modified polyimides a) **PI-1**, **azo-PI-1**; b) **PI-2**, **azo-PI-2**; and c) **PI-3**, **azo-PI-3** at room temperature.

Table 2. Viscosity, density, and *d*-spacing of (azo)polyimides.

Polymer code	Viscosity [dL/g]	Density [cm^3/g]	*d*-spacing [Å]
PI-1	0.42	1.04	5.14
azo-PI-1	0.42	1.41	4.97
PI-2	0.64	1.66	5.56
azo-PI-2	0.64	1.53	5.71
PI-3	0.67	1.71	5.75
azo-PI-3	0.51	1.58	5.94

Wide-angle X-ray diffraction (WAXD) patterns of azo-PIs exhibited typical characteristics for amorphous materials, showcasing broad diffraction peaks of the diffusion type in the range of 10–20° and an absence of a crystalline phase (Figure 3). The PIs' data has been previously presented in our earlier works [43, 44]. The *d*-spacing values, indicative of the average interchain distances in the polymer, were determined from the maximum position utilizing Bragg's law. Analysis of the data in Table 2 reveals that polymers derived from 6FDA dianhydride exhibit the highest d-spacing values, ranging from 5.56 to 5.94 Å. These values result from chain separation through CF) bulk groups [45]. Conversely, (azo)polyimides containing an ether linkage exhibit the smallest chain spacing, measuring between 4.97 and 5.14 Å, indicating better packing of the polymer chains. Solubility testing of the (azo)polyimides involved dissolving 10 mg of the polymer in 1 mL of

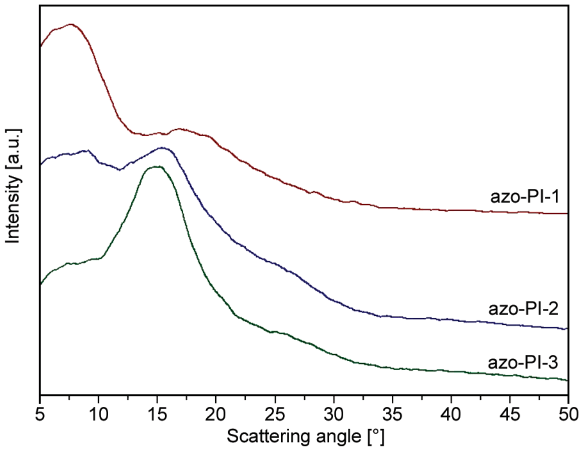

Figure 3. Wide-angle X-ray diffraction patterns of the obtained azo polyimides.

organic solvent. All samples displayed good solubility in DMSO and were partially soluble in THF and cyclohexanone under heat. The polymers were insoluble in $CHCl_3$, except for **azo-PI-1** and **azo-PI-3**. It is well-established that a higher content of flexible ether linkages in a polyimide structure or the presence of azo side groups enhances solubility [46].

3.2. Thermal characterization

Thermal properties of the obtained (azo)polyimides were investigated using differential scanning calorimetry (DSC) and thermogravimetric analysis (TGA). The investigated data are collected in Table 3. Azo PIs were prepared based on three polymer matrices with glass transition temperatures (T_g) exceeding 210 °C. The incorporation of azo moieties into the polymer structure led to a reduction in T_g compared to the precursors, attributed to the plasticization effect [47, 48]. Nevertheless, azo polyimides exhibited T_g values above 170 °C, ensuring high thermal stability of the photoinduced effects [49]. Poly(hydroxy imide)s typically undergoes two or three degradation steps. The first, observed in the range of 429–530 °C, is indicative of the thermal conversion of polyimides with OH groups in the ortho position to polybenzoxazole due to thermal rearrangement [50]. The second and third degradation steps, occurring in the range of 527–655 °C, are characteristic of the degradation of the main body of the polymer backbone. In contrast, azo polyimides displayed three or four degradation steps. The first step, in the range of 241–353 °C, is associated with the scission of azo moieties. The temperature of the maximum decomposition (T_{max}) of pure 4-[4-(6-hydroxyhexyloxy)phenylazo]pyridine is 333 °C [39]. The poly(hydroxy imide) matrices were not fully substituted by an azo chromophore, resulting in the observation of thermal conversion to polybenzoxazole as a degradation step at approximately 399 °C. Decomposition temperatures in the range of 452–657 °C are characteristic of the degradation of the polymer backbone [51]. All (azo)polyimides exhibited residual weight at 800 °C in the range of 45–51%.

3.3. Optical properties

The optical properties of azo polyimides were investigated in NMP solution ($c = 10^{-5}$ mol/L) and film. Both solutions and films were shielded from light for at least 24 h to prevent *trans*-*cis* isomerization of azo chromophores. Polyimide precursors utilized for the synthesis of azo polyimides exhibited two absorption bands at 260 and 300 nm in NMP solution (black curves in Figure 4). The chemical structure of the polymer backbone did not influence the character of the spectra. Substituting hydroxyl groups with azo chromophores introduced a new absorption band in the range of approximately 325–400 nm, characteristic of π–π^* transitions of the *trans*-isomer, representing 100% of the content of the *trans*-form in the sample (black curves in Figure 4). The UV-Vis spectra of the azo polyimide films were bathochromically shifted (approximately 7 nm) compared to the NMP solution (red curves in Figure 4).

The chromophore loading level of the polymers was determined using UV–Vis spectroscopy and the Lambert-Beer law [52]. The procedure was described in detail in the Experimental section. The degree of chromophore substitution in the polymer was calculated using calibration curves derived from the UV-Vis spectra of dilute solutions of the chromophore with various concentrations, specifically for 4-[4-(6-hydroxyhexyloxy)phenylazo]pyridine.

Table 3. Thermal properties of (azo)polyimides.

Sample	DSC	TGA (powder)			Residual weight[d] [%]
	T_g (powder) [°C]	T_5[a] [°C]	T_{10}[b] [°C]	T_{max}[c] [°C]	
PI-1	225	348	431	429; 527	48
azo-PI-1	176	324	370	349; 397; 452; 610	25
PI-2	214	318	470	465; 530; 655	45
azo-PI-2	204	295	365	353; 399; 535; 657	46
PI-3	226	447	495	530; 630	51
azo-PI-3	195	339	473	241; 537; 630	49

[a] Decomposition temperature of 5% weight loss.
[b] Decomposition temperature of 10% weight loss.
[c] Temperature of the maximum decomposition rate by derivative thermogravimetry (DTG).
[d] Residual weight at 800 °C in nitrogen.

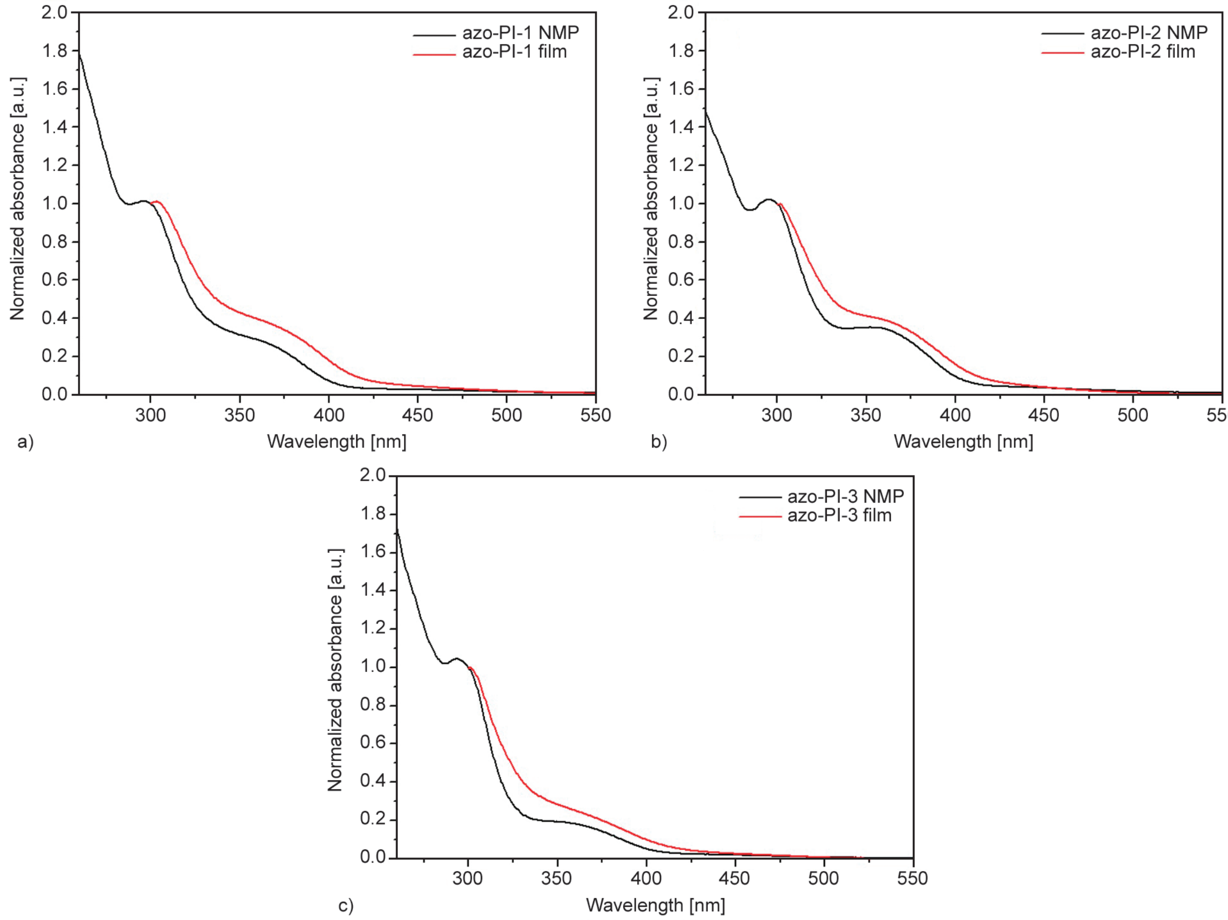

Figure 4. Normalized UV-Vis curves for a) **azo-PI-1**, b) **azo-PI-2**, c) **azo-PI-3** in NMP solution ($c = 10^{-5}$ mol/L) and polymer films.

By comparing the peak absorbance of the polymer in solution with a known concentration to the calibration curve, the degree of functionalization was estimated. The results indicated a degree of functionalization of 18% for **azo-PI-1**, 35% for **azo-PI-2**, and 7% for **azo-PI-3**.

3.4. Dark *cis-trans* isomerization

The investigation of dark *cis-trans* isomerization was conducted on azo polymer films prepared by pouring 0.2 mL of polymer solution onto a glass substrate (2×2 cm). Residual solvent was eliminated from the films by initially drying them at 100 °C for 2 h, followed by heating under vacuum conditions at 100 °C for an additional 24 h. This procedure resulted in the formation of thin polymer films (approximately 350 nm). The prepared samples were left in the dark for at least 24 h. Efficiency studies of *trans-cis* isomerization and dark *cis-trans* relaxation were performed as follows: Absorption spectra of the polyimide films were recorded before exposure to the excitation beam at room temperature to monitor differences in absorption arising from *trans-cis* photoconversion and the subsequent dark *cis-trans* back reaction. *Cis*-isomers were generated by irradiating the films with a 405 nm diode-laser light (intensity $I = 100$ mW/cm^2) until reaching the photostationary state. The photostationary state was achieved after 5 min of light exposure. Extending the exposure time to UV light did not affect the character of the UV-Vis spectra. Subsequently, UV-Vis spectra of the polymer layers were recorded immediately after switching off the UV light. The dark *cis-trans* reaction was monitored at room temperature from 30 min up to 6 days after switching off the excitation light.

Non-irradiated azo polyimides exhibited an absorption area in the range of 300–550 nm with maximum absorptions (λ_{max}) at 358 nm attributed to the *trans*-isomer of the azo chromophore, and at 300 nm corresponding to the main chain of the polymer backbone (black curves in Figure 5). Exposure of azo polyimide films to 405 nm laser light resulted in a reduction in intensity of the absorption band in the

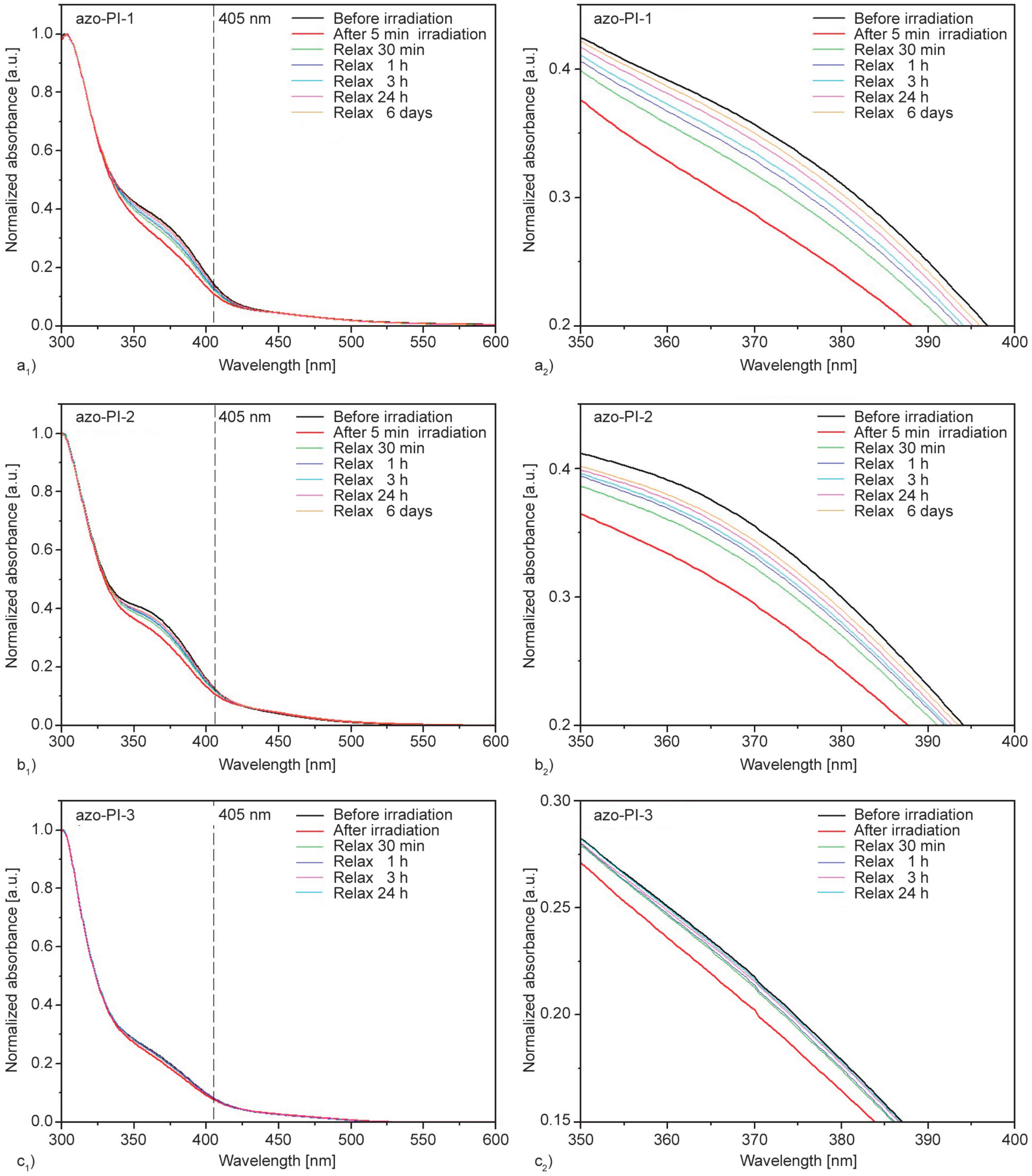

Figure 5. Normalized curves of *cis*-*trans* isomerization for a$_1$), a$_2$) **azo-PI-1**, b$_1$), b$_2$) **azo-PI-2**, and c$_1$), c$_2$) **azo-PI-3**.

range of 325–400 nm and the formation of isosbestic points at approximately 426 nm (red curves in Figure 5). The changes in the UV-Vis spectra indicate the presence of *cis*- and *trans*-isomers in the sample. The application of 405 nm excitation light, located at the end of the right slope of the polymer absorption, excited the π–π* absorption transition. Azo polyimides exhibited similar UV-Vis absorption spectra, suggesting that the *cis*-isomer content and dynamics of *cis*-*trans* reactions primarily result from the chemical structures.

The efficiency of *trans* to *cis*-isomer photoconversion was determined by monitoring the change in absorbance at the wavelength corresponding to the absorption maximum of the *trans*-form, before and immediately after light irradiation. The *cis*-isomer content was calculated using Equation (1) [53]. Specifically, the *cis*-isomer content was found to be

15, 14, and 5% for **azo-PI-1**, **azo-PI-2**, and **azo-PI-3**, respectively. The observed low photoresponse of the azo polyimides may be attributed to the positioning of the excitation beam relative to the maximum absorption of the polymer. Considering the influence of the chemical structure of the polymer main chain, it is evident that ether groups enhance the photoresponse compared to CF_3 moieties. The *cis*-isomer content was comparable for **azo-PI-1** and **azo-PI-2**, even though the hydroxyl group substitution by the azo group was almost twice as high for **azo-PI-2**. In the case of the copolyimide **azo-PI-3**, which incorporated an additional repeated unit (synthesized from 6FDA and 4MPD), the *trans*-*cis* conversion was notably lower reaching only 5%.

In Figure 6, the dynamic of *cis*-*trans* isomerization is depicted as the decrease in the normalized content of *cis*-isomer over time. Changes in the absorption spectra were monitored for up to 6 days, revealing a complete return to the *trans*-form only for **azo-PI-3**, achieved after 24 h of relaxation. The observed fast *cis*-*trans* conversion of **azo-PI-3** may result from the highest *d*-spacing value (5.94 Å), guaranteeing a larger free volume necessary for *cis*-*trans* isomerization and the low content of azo chromophore in the polymer structure. In azo-rich "side-chain" polymers where the chromophores are located close to each other, the thermal isomerization can be hindered by π–π interactions between *cis*-isomers [54–56]. For that reason, dark relaxation for **azo-PI-2** is longer than for **azo-PI-1**, despite the higher *d*-spacing value of **azo-PI-2** (cf. Table 2). Similar behaviour was observed for side-chain poly(ether imide)s with 4-[4-(6-hydroxyhexyloxy)phenylazo]pyridine [56].

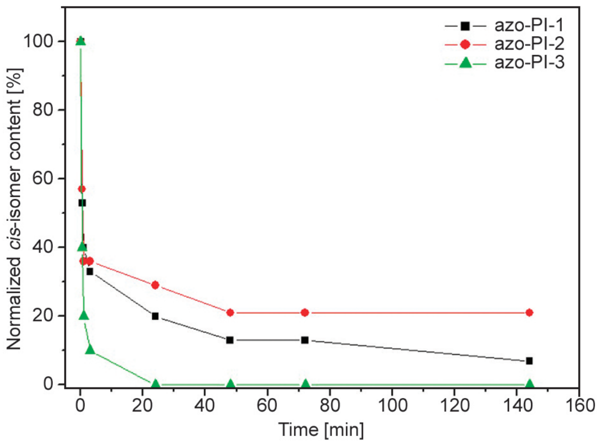

Figure 6. Dynamic of *cis-trans* isomerization in the function of time for azo polyimides.

3.5. Photomechanical effect

The photomechanical effect of the side-chain azo polyimides was investigated using a 405 nm diode laser beam (intensity, $I = 100$ mW/cm^2). The cantilevers were illuminated by the beam with linear polarization in a direction parallel to the long axis of the samples for 1 h. Based on previous studies, the parallel polarization of the laser light resulted in the chromophore ordering in perpendicular directions, leading to contractions of the sample along a vertical direction. Consequently, bending towards the laser source was observed [32]. The dimensions of the cantilevers were 1 mm (width) × 5 mm (length) × ~35 µm (thickness).

Figure 7 presents the position of the blank samples with no azo chromophore in the chemical structure in the initial state, during the 405 nm-light irradiation, and after laser exposition. As can be seen, blank samples do not show the photomechanical effect.

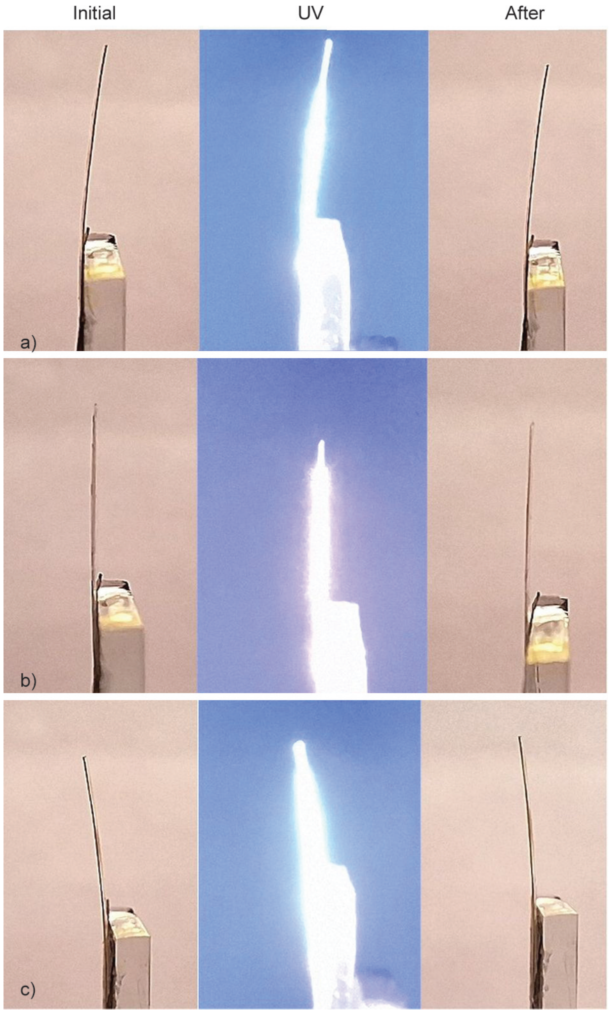

Figure 7. 405 nm-light irradiation of blank samples a) **PI-1**, b) **PI-2**, and c) **PI-3**. Polarization of light, E||x, total irradiation time 1 h, the laser beam propagation direction is from left to right.

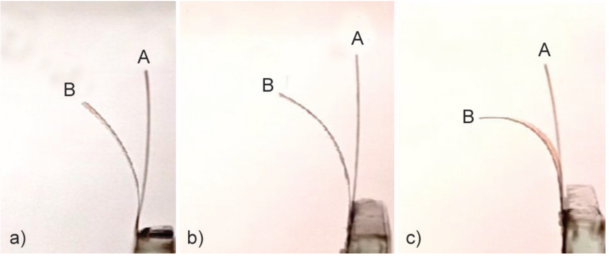

Figure 8. Bending of cantilevers for a) **azo-PI-1**, b) **azo-PI-2**, and c) **azo-PI-3**, where position "A" is the initial state, position "B" is after 1h of 405 nm light irradiation, polarization E||x. The laser beam propagation direction is from left to right.

Their position is the same before and after polarized light exposition.

The bending angle was assessed based on Figure 8 and Figure 9, created by superimposing two photos (in the initial state and immediately after turning off the excitation light) in a graphics program. The bending angle was approximately 30°, 35°, and 40° for **azo-PI-1**, **azo-PI-2**, and **azo-PI-3**, respectively (Figure 8). Using the horizontally polarized light right-direction bending was observed, but the bending angle was lower than for vertical polarization (Figure 9). This observation proves the photomechanical mechanism of cantilever deformation [34]. Azo polyimides with bulky CF_3 groups exhibited higher bending angles than **azo-PI-1** with ether and CH_3 groups in the main chain. Other azo polyimides with bulky CF_3 or "cardo" groups reported in the literature demonstrated a significantly better photomechanical response than CH_3 groups [22]. The photomechanical response increased with the increasing value of the *d*-spacing, resulting in the largest average interchain distances. The copolyimide **azo-PI-3**, with the highest value of the *d*-spacing (5.94 Å), exhibited the most significant photomechanical response. Considering literature reports, the bending angles for "side-chain" azo polyimides presented in this work, falling in the range of 30–40°, are relatively high. In a previous paper [38], the maximum bending angle reached for the "side-chain" was 70°, but the foils were thinner (~20 µm), and azobenzene groups were attached to each polymer repeat unit. In this study, the largest photoresponse of a cantilever was observed for **azo-PI-3** with only 7% hydroxyl group substitution. Increasing the bending angle of the cantilevers can be achieved by adjusting the length of the excitation beam towards the higher absorption range of the azo polymers. The utilized 405 nm excitation light was positioned on the right slope of the absorption range of the studied azo polyimides. The obtained bending angles are relatively high considering the thickness of the samples. However, it is worth noting that increasing the thickness reduces the magnitude of the bending angle. The largest photomechanical response is observed for 20 µm foils and thinner [33]. From the perspective of practical applications of photoactive foils, maximizing the polymer thickness is desirable, as thin foils are more susceptible to mechanical damage.

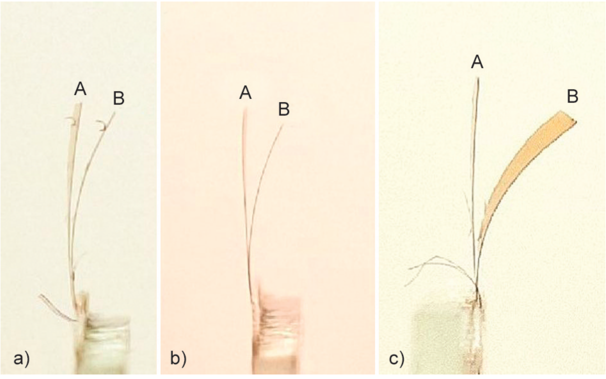

Figure 9. Bending of cantilevers for a) **azo-PI-1**, b) **azo-PI-2**, and c) **azo-PI-3**, where position "A" is the initial state, position "B" is after 1h of 405 nm light irradiation, polarization E||x. The laser beam propagation direction is from left to right.

No relaxation of any of the cantilevers to their original position was observed even after 12 months of irradiation. Figure 10 illustrates the absence of a difference in the position of the bending cantilever. The figure was generated by superimposing two photos (taken immediately after turning off the excitation light and after 12 months of dark relaxation) in a graphics program. Despite many papers describing the photomechanical effects in amorphous azo polyimides, there is no information available regarding

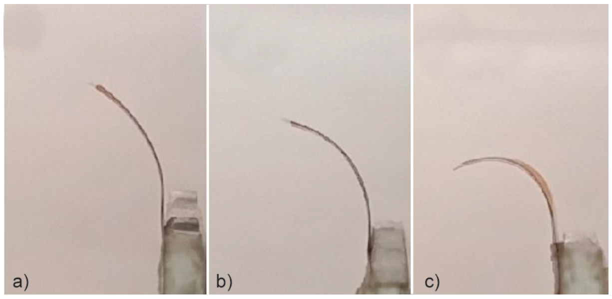

Figure 10. Photos of a) **azo-PI-1**, b) **azo-PI-2**, and c) **azo-PI-3** cantilevers, directly after 405 nm-light irradiation and after 12 months of dark relaxation. The figure was created by superimposing two photos (immediately after turning off the excitation light and after 12 months of dark relaxation).

the relationship between *cis*-*trans* isomerization and the unbending process [9, 20–23, 25–38]. We suppose that the high return stability observed may be attributed to the chemical structure of the azo polyimides. Based on literature reports, it can be concluded that the manner of attaching the azo dye to the polymer backbone plays a significant role in the thermal unbending of polyimide cantilevers compared to *cis-trans* isomerization. For "main-chain" azo polyimides, relaxation of the cantilevers to their original position was observed within 75 s to 10 days, depending on the rigidity of the polymer structure [21, 27]. "T-type" azo polyimides showed stability in bending for more than 10 days after irradiation [35], while for "guest-host" polyimide cantilevers, no unbending was observed even after 3 months following the cessation of excitation light [36, 37]. Considering the type of azo chromophore attachment, it is evident that the incorporation of azo moieties as a part of the main chain of the polymer structure results in relatively fast unbending to the initial position. The presence of azo groups in the macromolecular chain results in a large polymer sensitivity to chromophore *cis*-*trans* reorientation. Azo groups located in the main chain can easily push the whole macromolecule during the azobenzene reorientation process, thereby causing the unbending process to occur. In the case of polymers where azo groups are in the side chain of the polymer structure ("T-type" polymers, side-chain polymers) or where the dye is dispersed in the polymer matrix, the unbending process is significantly longer or not observed, as demonstrated. The presence of the N=N bond away from the main chain of the macromolecule causes the isomerization of the chromophore to take place outside the macromolecule. For this reason, the isomerization of the azo chromophore is not "noticeable" to the polymer chain. Its position changes only slightly, and the unbending process takes much longer than in the case of main-chain polymers. The large stability of the side-chain cantilevers proves advantageous from an application standpoint. In various photoactive devices, the persistence of bending is imperative until the initiation of the unbending process, which may be induced by an alteration in wavelength or polarization of the excitation light.

4. Conclusions

The newly synthesized amorphous polyimides, functionalized in the side chain with azo pyridine groups, demonstrated both high thermal stability and efficient photomechanical response. A crucial observation in this study is that, despite the low substitution of polymer hydroxyl groups (7–35%) and a low content of *cis* isomer (up to 15%), an effective photomechanical response was achieved. Azo polyimide cantilevers exhibited bending angles in the range of 30–40°. The photogenerated movement of the cantilevers is primarily dependent on the polymer backbone structure, with the flexibility of the polymer main chain playing a dominant role in the bending of the cantilevers. Polymers with bulky CF_3 moieties displayed higher bending angles and faster *cis*-*trans* dark relaxation than polyimides with ether groups. The more flexible backbone of copolyimides contributed to the largest photomechanical effect, despite the lowest content of the azo group. The studied polymer foils exhibited high stability in bending, with no relaxation of any of the cantilevers to their original position observed even 12 months after turning off the excitation light.

Acknowledgements

This research was funded by the National Science Centre, Poland, grant number UMO-2019/35/D/ST5/00533. The authors thank Dr Mariola Siwy for measurements of FTIR and *cis*-*trans* isomerization.

References

[1] Zhuang Y., Seong J. G., Lee Y. M.: Polyimides containing aliphatic/alicyclic segments in the main chains. Progress in Polymer Science, **92**, 35–88 (2019). https://doi.org/10.1016/j.progpolymsci.2019.01.004

[2] Diaham S.: Polyimide in electronics: Applications and processability overview. in 'Polyimide for electronic and electrical engineering applications' (ed.: Diaham S.) IntechOpen, London, 1–4 (2021). https://doi.org/10.5772/intechopen.92629

[3] Wie J. J.: Photomechanical effects in amorphous and semicrystalline polymers. in 'Photomechanical materials, composites, and systems: Wireless transduction of light into work' (ed.: White T. J.) Wiley, Hoboken, Vol. 4, 117–152 (2017). https://doi.org/10.1002/9781119123279.ch4

[4] Todorov T., Nikolova L., Tomova N.: Polarization holography. 1: A new high-efficiency organic material with reversible photoinduced birefringence. Applied Optics, **23**, 2858–2866 (1984). https://doi.org/10.1364/AO.23.004309

[5] Dumont M., Sekkat Z.: Dynamical study of photoinduced anisotropy and orientational relaxation of azo dyes in polymeric films: Poling at room temperature. in ‘Proceedings of SPIE 1774, Nonconducting Photopolymers and Applications, San Diego, USA) 188–199 (1993).
https://doi.org/10.1117/12.139169

[6] Rochon P., Batalla E., Natansohn A.: Optically induced surface gratings on azoaromatic polymer films. Applied Physics Letters, **66**, 136–138 (1995).
https://doi.org/10.1063/1.113541

[7] Kim D. Y., Tripathy S. K., Li L., Kumar J.: Laser-induced holographic surface relief gratings on nonlinear optical polymer films. Applied Physics Letters, **66**, 1166–1168 (1995).
https://doi.org/10.1063/1.113845

[8] White T. J.: Photomechanical effects in liquid crystalline polymer networks and elastomers. Journal of Polymer Science Part B: Polymer Physics, **56**, 695–705 (2018).
https://doi.org/10.1002/polb.24576

[9] Wie J. J., Wang D. H., Lee K. M., White T. J., Tan L-S.: The contribution of hydrogen bonding to the photomechanical response of azobenzene-functionalized polyamides. Journal of Materials Chemistry C, **6**, 5964 (2018).
https://doi.org/10.1039/C8TC00319J

[10] Si Q., Feng Y., Yang W., Fu L., Yan Q., Dong L., Long P., Feng W.: Controllable and stable deformation of a self-healing photo-responsive supramolecular assembly for an optically actuated manipulator arm. ACS Applied Materials and Interfaces, **10**, 29909–29917 (2018).
https://doi.org/10.1021/acsami.8b08025

[11] Gelebart A. H., Mulder D. J., Varga M., Konya A., Vantomme G., Meijer E. W., Selinger R. L. B., Broer D. J.: Making waves in a photoactive polymer film. Nature, **546**, 632–636 (2017).
https://doi.org/10.1038/nature22987

[12] Shankar M. R., Smith M. L., Tondiglia V. P., Lee K. M., McConney M. E., Wang D. H., Tan L-S., White T. J.: Contactless, photoinitiated snap-through in azobenzene-functionalized polymers. Proceedings of the National Academy of Sciences, **110**, 18792–18797 (2013).
https://doi.org/10.1073/pnas.1313195110

[13] Cheng F., Yin R., Zhang Y., Yen C-C., Yu Y.: Fully plastic microrobots which manipulate objects using only visible light. Soft Material Journal, **6**, 3447–3449 (2010).
https://doi.org/10.1039/C0SM00012D

[14] Palffy-Muhoray P.: Printed actuators in a flap. Nature Materials, **8**, 614–615 (2009).
https://doi.org/10.1038/nmat2502

[15] Lee J., Oh S., Pyo J., Kim J-M., Je J. H.: A light-driven supramolecular nanowire actuator. Nanoscale, **7**, 6457–6461 (2015).
https://doi.org/10.1039/C5NR01118C

[16] Dradrach K., Rogóż M., Grabowski P., Xuan C., Węgłowski R., Konieczkowska J., Schab-Balcerzak E., Piecek W., Wasylczyk P.: Traveling wave rotary micromotor based on a photomechanical response in liquid crystal polymer networks. ACS Applied Materials and Interfaces, **12**, 8681–8686 (2020).
https://doi.org/10.1021/acsami.9b20309

[17] van Oosten C. L., Bastiaansen C. W. M., Broer D. J.: Printed artificial cilia from liquid-crystal network actuators modularly driven by light. Nature Materials, **8**, 677–682 (2009).
https://doi.org/10.1038/nmat2487

[18] Serak S., Tabiryan N., Vergara R., White T. J., Vaia R. A., Bunning T. J.: Liquid crystalline polymer cantilever oscillators fueled by light. Soft Material Journal, **6**, 779–783 (2010).
https://doi.org/10.1039/B916831A

[19] Kitagawa D., Kobatake S.: Photoreversible current ON/OFF switching by the photoinduced bending of gold-coated diarylethene crystals. Chemical Communication Journal, **51**, 4421–4424 (2015).
https://doi.org/10.1039/C5CC00355E

[20] Wie J. J., Wang D. H., Lee K. M., Tan L-S., White T. J.: Molecular engineering of azobenzene-functionalized polyimides to enhance both photomechanical work and motion. Chemistry of Materials, **26**, 5223–5230 (2014).
https://doi.org/10.1021/cm5018757

[21] Wie J. J., Wang D. H., Tondiglia V. P., Tabiryan N. V., Vergara-Toloza R. O., Tan L-S., White T. J.: Photopiezoelectric composites of azobenzene-functionalized polyimides and polyvinylidene fluoride. Macromolecular Rapid Communications, **35**, 2050–2056 (2014).
https://doi.org/10.1002/marc.201400455

[22] Baczkowski M. L., Wang D. H., Lee D. H., Lee K. M., Smith M. L., White T. J., Tan L-S.: Photomechanical deformation of azobenzene-functionalized polyimides synthesized with bulky substituents. ACS Macro Letters, **6**, 1432–1437 (2017).
https://doi.org/10.1021/acsmacrolett.7b00854

[23] Lee K. M., Wang D. H., Koerner H., Vaia R. A., Tan L-S., White T. J.: Enhancement of photogenerated mechanical force in azobenzene-functionalized polyimides. Angewandte Chemie International Edition, **51**, 4117–4121 (2012).
https://doi.org/10.1002/anie.201200726

[24] Hosono N., Yoshikawa M., Furukawa H., Totani K., Yamada K., Watanabe T., Horie K.: Photoinduced deformation of rigid azobenzene-containing polymer networks. Macromolecules, **46**, 1017–1026 (2013).
https://doi.org/10.1021/ma302157u

[25] Lee K. M., Wang D. H., Koerner H., Vaia R. A., Tan L-S., White T. J.: Photomechanical response of pre-strained azobenzene-functionalized polyimide materials. Macromolecular Chemistry and Physics, **214**, 1189–1194 (2013).
https://doi.org/10.1002/macp.201200340

[26] Lee K. M., Koerner H., Wang D. H., Tan L-S., White T. J., Vaia R. A.: Tailoring the photomechanical response of glassy, azobenzene-functionalized polyimides by physical aging. Macromolecules, **45**, 7527–7534 (2012). https://doi.org/10.1021/ma3016085

[27] Wang D. H., Wie J. J., Lee K. M., White T. J., Tan L-S.: Impact of backbone rigidity on the photomechanical response of glassy, azobenzene-functionalized polyimides. Macromolecules, **47**, 659–667 (2014). https://doi.org/10.1021/ma402178z

[28] Wie J. J., Chatterjee S., Wang D. H., Tan L-S., Shankar M. R., White T. J.: Azobenzene-functionalized polyimides as wireless actuators. Polymer, **55**, 5915–5923 (2014). https://doi.org/10.1016/j.polymer.2014.06.084

[29] Wang D. H., Lee K. M., Lee D. H., Baczkowski M., Lee J. G., Wie J. J., Tan L-S.: Intermolecular interactions and intramolecular motions in photomechanical effect: Nonlinear thermo- and photomechanical behaviors of azobenzene-functionalized amide–imide block copolymers. ACS Applied Materials and Interfaces, **13**, 48127–48140 (2021). https://doi.org/10.1021/acsami.1c14511

[30] Wang D. H., Lee K. M., Lee D. H., Baczkowski M., Park H., McConney M. E., Tan L-S.: Role of alicyclic conformation-isomerization in the photomechanical performance of azobenzene-functionalized cross-linked polyimides containing tetra-substituted cyclohexane moieties. ACS Macro Letters, **10**, 278–283 (2021). https://doi.org/10.1021/acsmacrolett.0c00903

[31] Zhang P., Lan Z., Wei J., Yu Y.: Photodeformable azobenzene-containing polyimide with flexible linkers and molecular alignment. ACS Macro Letters, **10**, 469–475 (2021). https://doi.org/10.1021/acsmacrolett.1c00040

[32] Wang D. H., Lee K. M., Yu Z., Koerner H., Vaia R. A., White T. J., Tan L-S.: Photomechanical response of glassy azobenzene polyimide networks. Macromolecules, **44**, 3840–3846 (2011). https://doi.org/10.1021/ma200427q

[33] Wang D. H., Lee K. M., Koerner H., Yu Z., Vaia R. A., White T. J., Tan L-S.: Flexural-torsional photomechanical responses in azobenzene-containing crosslinked polyimides. Macromolecular Materials and Engineering, **297**, 1167–1174 (2012) https://doi.org/10.1002/mame.201200240

[34] Beery D., Stanisauskis E., McLeod G. M., Das A., Guillory G. A., Kennemur J. G., Oates W. S., Hanson K.: Enabling lower energy light harvesting in stilbene-based photomechanical polymers via triplet sensitization. ACS Applied Polymer Materials, **4**, 4081–4086 (2022). https://doi.org/10.1021/acsapm.2c00660

[35] Kozanecka-Szmigiel A., Schab-Balcerzak E., Szmigiel D., Konieczkowska J.: The unexpected photomechanical effect in glassy “T-type” azopolyimides. Journal of Materials Chemistry C, **7**, 4032–4037 (2019). https://doi.org/10.1039/C8TC06518G

[36] Li S., Feng Y., Wang W., Ji T., Han J., Long P., Cao C., Feng W.: Polarization-induced alignment of azobenzene/fluorinated polyimide for three-dimensional shape-persistent and photo-responsive elastic helixes. Computer Science and Information Technology, **169**, 158–166 (2019). https://doi.org/10.1016/j.compscitech.2018.11.014

[37] Konieczkowska J., Bujak K., Nocoń K., Schab-Balcerzak E.: The large and stable photomechanical effect in the glassy guest-host azopolymers. Dyes Pigments, **171**, 107659 (2019). https://doi.org/10.1016/j.dyepig.2019.107659

[38] Sun X., Wei J., Yu Y.: Photoinduced deformation of amorphous polyimide enabled by an improved azobenzene isomerization efficiency. Polymer Chemistry, **13**, 5447–5452 (2022). https://doi.org/10.1039/D2PY00691J

[39] Bujak K., Orlikowska H., Małecki J. G., Schab-Balcerzak E., Bartkiewicz S., Bogucki J., Sobolewska A., Konieczkowska J.: Fast dark *cis-trans* isomerization of azopyridine derivatives in comparison to their azobenzene analogues: Experimental and computational study. Dyes Pigments, **160**, 654–664 (2019). https://doi.org/10.1016/j.dyepig.2018.09.006

[40] Konieczkowska J., Kozanecka-Szmigiel A., Bujak K., Szmigiel D., Małecki J. G., Schab-Balcerzak E.: Photoresponsive behaviour of “T-type” azopolyimides. The unexpected high efficiency of diffraction gratings, modulations and stability of the SRG in azopoly(ether imide). Materials Science and Engineering B, **273**, 115387 (2021). https://doi.org/10.1016/j.mseb.2021.115387

[41] Schab-Balcerzak E., Konieczkowska J., Siwy M., Sobolewska A., Wojtowicz M., Wiacek M.: Comparative studies of polyimides with covalently bonded azodyes with their supramolecular analoges: Thermo-optical and photoinduced properties. Optical Materials, **36**, 892–902 (2014). https://doi.org/10.1016/j.optmat.2013.12.017

[42] Nocoń-Szmajda K., Jankowski A., Wolińska-Grabczyk A., Konieczkowska J.: Guest-host and functionalized side-chain azopolyimide membranes for controlled gas separation. Polymer, **229**, 124012 (2021). https://doi.org/10.1016/j.polymer.2021.124012

[43] Nocoń-Szmajda K., Wolińska-Grabczyk A., Jankowski A., Szeluga U., Wójtowicz M., Konieczkowska J., Hercog A.: Gas transport properties of mixed matrix membranes based on thermally rearranged poly(hydroxyimide)s filled with inorganic porous particles. Separation and Purification Technology, **242**, 116778 (2020). https://doi.org/10.1016/j.seppur.2020.116778

[44] Nocoń-Szmajda K., Wolińska-Grabczyk A., Jankowski A., Dryzek J., Dryzek E., Janeczek H., Grabiec E., Musioł M.: Effects of ionic liquid doping on gas transport properties of thermally rearranged poly(hydroxyimide)s. Separation and Purification Technology, **254**, 117664 (2021).
https://doi.org/10.1016/j.seppur.2020.117664

[45] Jankowski A., Grabiec E., Nocon-Szmajda K., Marcinkowski A., Janeczek H., Wolinska-Grabczyk A.: Polyimide-based membrane materials for CO_2 separation: A comparison of segmented and aromatic (*co*)polyimides. Membranes, **11**, 274 (2021).
https://doi.org/10.3390/membranes11040274

[46] Konieczkowska J., Wojtowicz M., Sobolewska A., Noga J., Jarczyk-Jedryka A., Kozanecka-Szmigiel A., Schab-Balcerzak E.: Thermal, optical and photoinduced properties of a series of homo and *co*-polyimides with two kinds of covalently bonded azo-dyes and their supramolecular counterparts. Optical Materials, **48**, 139–149 (2015).
https://doi.org/10.1016/j.optmat.2015.07.033

[47] Konieczkowska J., Kozanecka-Szmigiel A., Janeczek H., Małecki J., Wójtowicz M., Schab-Balcerzak E.: No effect of the hydrogen bonds on the physicochemical properties of the guest-host poly(amide imide) azosystems and efficiency of chromophore orientation. Dyes Pigments, **156**, 250–259 (2018).
https://doi.org/10.1016/j.dyepig.2018.04.017

[48] Konieczkowska J., Janeczek H., Małecki J., Trzebicka B., Szmigiel D., Kozanecka-Szmigiel A., Schab-Balcerzak E.: Noncovalent azopoly(ester imide)s: Experimental study on structure-property relations and theoretical approach for prediction of glass transition temperature and hydrogen bond formation. Polymer, **113**, 53–66 (2017).
https://doi.org/10.1016/j.polymer.2017.02.044

[49] Guo R., Sanders D. F., Smith Z. P., Freeman B. D., Paul D. R., McGrath J. E.: Synthesis and characterization of thermally rearranged (TR) polymers: Effect of glass transition temperature of aromatic poly(hydroxyimide) precursors on TR process and gas permeation properties. Journal of Materials Chemistry A, **1**, 6063–6072 (2013).
https://doi.org/10.1039/C3TA10261K

[50] Tsutsumi N., Morishima M., Sakai W.: Nonlinear optical (NLO) polymers. 3. NLO polyimide with dipole moments aligned transverse to the imide linkage. Macromolecules, **31**, 7764–7769 (1998).
https://doi.org/10.1021/ma9803436

[51] Sava I., Sacarescu L., Stoica I., Apostol I., Damian V., Hurduc N.: Photochromic properties of polyimide and polysiloxane azopolymers. Polymer International, **58**, 163–170 (2009).
https://doi.org/10.1002/pi.2508

[52] Schab-Balcerzak E., Siwy M., Kawalec M., Sobolewska A., Chamera A., Miniewicz A.: Synthesis, Characterization, and study of photoinduced optical anisotropy in polyimides containing side azobenzene units. Journal of Physical Chemistry A, **113**, 8765–8780 (2009).
https://doi.org/10.1021/jp904250r

[53] Bujak K., Orlikowska H., Sobolewska A., Schab-Balcerzak E., Janeczek H., Bartkiewicz S., Konieczkowska J.: Azobenzene vs azopyridine and matrix molar masses effect on photoinduced phenomena. European Polymer Journal, **115**, 173–184 (2019).
https://doi.org/10.1016/j.eurpolymj.2019.03.028

[54] Dhanabalan A., Balogh D. T., Mendonça C. R., Riul A., Constantino C. J. L., Giacometti J. A., Zilio S. C., Oliveira O. N.: Mixed langmuir and langmuir–blodgett films of disperse red-13 dye-derivatized methacrylic homopolymer and cadmium stearate. Langmuir, **14**, 3614–3619 (2000).
https://doi.org/10.1021/la9800250

[55] García-Amorós J., Díaz-Lobo M., Nonell S., Velasco D.: Fastest thermal isomerization of an azobenzene for nanosecond photoswitching applications under physiological conditions. Angewandte Chemie International Edition, **51**, 12820–12823 (2012).
https://doi.org/10.1002/anie.201207602

[56] Konieczkowska J., Siwy M.: Comprehensive investigations of *trans-cis-trans* isomerization in the solid state for azo polyimides. Dyes Pigments, **219**, 111558 (2023).
https://doi.org/10.1016/j.dyepig.2023.111558